Wood Sci Technol
DOI 10.1007/s00226-010-0351-5

ORIGINAL

Application of micromechanical models to tensile properties of wood–plastic composites

Sébastien Migneault · Ahmed Koubaa · Fouad Erchiqui · Abdelkader Chaala · Karl Englund · Michael P. Wolcott

Received: 31 October 2009

Abstract Wood–plastic composites (WPC) were produced with white birch pulp fibers of different aspect ratios (length-to-diameter), high-density polyethylene, and using two common processes: extrusion or injection molding. Three additive levels were also used: no additive, compatibility agent, and process lubricant. Fiber size was measured with an optical fiber quality analyzer. Tensile properties of WPC were measured and modeled as a function of fiber aspect ratio. Models were fitted to experimental values using the minimum sum of squared error method. A shift from the oriented fiber case (injection molding) to the randomly oriented fiber case (extrusion) was achieved using a fiber orientation factor. Fiber/matrix stress transfer increased with increasing fiber aspect ratio. Stress transfer was reduced with the use of process lubricant. Unexpectedly, the compatibility agent had the same effect. Fiber strength and stiffness contributions to the composite were lower than those of intrinsic fiber properties.

S. Migneault
Centre de recherche sur le bois, Université Laval, Québec, QC G1V 0A6, Canada

A. Koubaa (✉) · F. Erchiqui
Université du Québec en Abitibi–Témiscamingue, 445 boul. de l'Université, Rouyn–Noranda, QC J9X 5E4, Canada
e-mail: ahmed.koubaa@uqat.ca

A. Chaala
Service de recherche et d'expertise en transformation des produits forestiers, 25 rue Armand–Sinclair, Amqui, QC G5J 1K3, Canada

K. Englund · M. P. Wolcott
Wood Materials and Engineering Laboratory, Washington State University, Pullman, WA 99164–1806, USA

Published online: 24 June 2010

Introduction

Fiber-reinforced polymers have been increasingly used in a variety of engineering applications since the 1960s (Gibson 2007). In recent years, interest has turned to the development of wood–plastic composites (WPC) (Clemons 2002; Rowell 2007; Smith and Wolcott 2006). The use of natural wood fibers as a reinforcement or filler has many advantages over synthetic fibers, such as abundant supply, low cost, biodegradability, high specific properties, low abrasiveness, and no health hazards. Disadvantages stem from the hygroscopic and polar nature of wood.

Analytical modeling is a simple and useful tool to predict and understand composite behavior as a function of its component characteristics (Gibson 2007). Effective analytical micromechanical models have been developed for synthetic short fiber-reinforced polymers (Gibson 2007). The most utilized and known theories for tensile properties are rule of mixtures (ROM), Cox model, Halpin-Tsai model, and Bowyer-Bader model (Gibson 2007; Kalaprasad et al. 1997). ROM are very simple models using fiber and matrix sum of volume weighted properties to predict composite property. ROM can be parallel or series. Hirsch model is a combination of parallel and series ROM. The Halpin-Tsai model considers matrix-to-fiber property ratio instead of sum of volume-weighted properties. The Cox model suggests that stress in fiber is proportional to the difference between fiber strain and the strain that matrix would have if there were no fibers. The Bowyer–Bader model considers the contribution of fibers below and above critical fiber length.

In a tensile loaded composite sample, stress is transferred from matrix to fiber by interfacial shear stress (τ) (Gibson 2007). The level of stress transferred depends, among others, on fiber-matrix interfacial adhesion quality and fiber orientation (Baïlon and Dorlot 2000; Beckermann and Pickering 2009; Gibson 2007). These concepts can be included to models by using reinforcement efficiency factor and orientation factor. Stress transferred to fiber increases as fiber length increases, until the stress transferred reaches intrinsic fiber resistance (Fig. 1). This length is called critical fiber length (L_c) (Baïlon and Dorlot 2000; Beckermann and Pickering 2009; Gibson 2007). Below L_c, fibers are pulled–out at the composite rupture, whereas above L_c, no more reinforcement is reached with further fiber-length increase.

Some authors have used analytical modeling for natural fiber-reinforced (or filled) polymers. Simonsen (1997) used ROM to model the bending modulus of elasticity of wood fiber–filled thermoplastics made with three different matrixes: polypropylene, polyethylene, and polystyrene. The ROM was fitted to experimental curves using a reinforcement efficiency factor. Factors found varied between 0.61 and 0.85, depending on the polymer matrix.

Some authors have used single fiber specimen to evaluate natural fiber reinforcement efficiency. Sretenovic et al. (2006) studied stress transfer mechanisms in wood fiber/polyethylene single fiber specimens and showed that the stress transfer in WPC follows the classical "shear lag" theory. Herra-Franco and Valadez-González (2005) used pull–out tests on henequen/polyethylene single fiber specimens and found that critical length and interfacial shear stress varied with fiber aspect ratio and fiber/matrix adhesion quality. Doan et al. (2006) modeled the

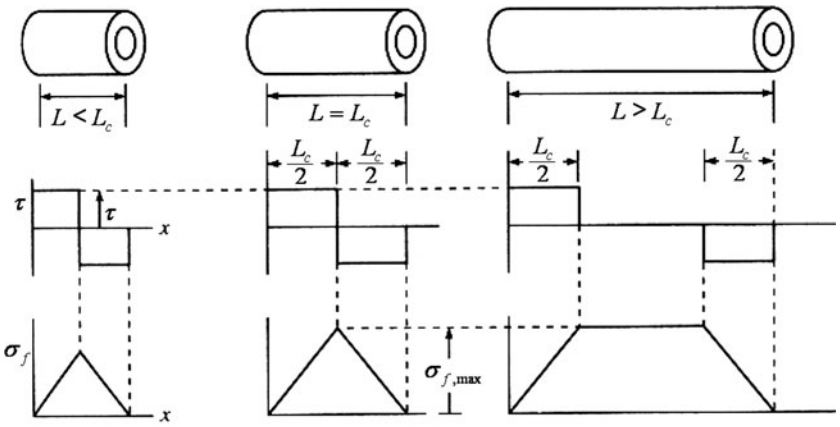

Fig. 1 Effect of fiber length on stress transferred from matrix to fibers in a short fiber composite according to the Kelly–Tyson model (Adapted from Gibson 2007)

tensile properties of injection molded jute/polypropylene composites as a function of fiber volume fraction using ROM. Fiber/matrix interfacial shear stress was obtained from single fiber pull–out tests and was incorporated into the tensile strength model. A loss factor for fiber orientation was used to fit the model to experimental values. Orientation factors found varied from 0.1 to 0.36. A loss factor for stress transfer efficiency was used for the composite modulus of elasticity. Factors varied from 0.42 to 0.51. The models give a good fit to experimental values.

Some authors incorporated natural fiber characteristics into models. Beckermann and Pickering (2009) determined L_c and τ for hemp single fiber/polypropylene composite. Values found were 0.83 mm for L_c and 15.4 MPa for τ. They prepared a composite made of 40 mass proportion hemp fibers and polypropylene and modeled its tensile strength using the Bowyer–Bader model. Length distribution of fibers extracted from the composite was measured and incorporated into model. Experimental strength value was one-third of model prediction, mainly because of fiber orientation. An orientation factor of 0.34 was found, suggesting a planar-random fibre arrangement. Marklund et al. (2008) included two fundamental wood fiber characteristics into WPC stiffness models: their orthotropic nature and hollow shape (lumens). Error introduced by neglecting the orthotropic nature of fiber cell wall could reach 10–20%. This error is larger for higher fiber volume fraction and resin-filled lumens. Neagu et al. (2006) used the Hashin and Rosen micromechanical composite model and the theory of classical laminate mechanics to evaluate the contribution of various fibers to WPC tensile modulus of elasticity. Fiber orientation distribution was measured using image analysis and incorporated into the models. Many commonly used fibers in the pulp and paper industry were screened. It was concluded that the stiffness contribution of fibers varies according to fiber treatment, such as pulping process, pulp yield, and bleaching. Fiber length was not considered in the models.

Although effective micromechanical models have been developed and used for synthetic short fiber-reinforced polymers (Gibson 2007), there was very little

information available on the effectiveness of these models for WPC. Most of previous research considered fiber volume fraction or fiber/matrix interface shear stress, not wood fiber characteristics. Incorporating fundamental wood fiber characteristics into models would allow a better understanding of the influence of fiber characteristics on the macroscopic behavior of WPC. Thus, the objective of this study was to model the tensile properties of WPC as a function of fiber aspect ratio (length/diameter) under different conditions.

Models

The rule of mixtures (ROM) states that the property of a composite is equal to the sum of the volume-weighted property of its component materials (Baïlon and Dorlot 2000; Gibson 2007). ROM is given in Eq. 1, where v is the volume fraction, and P is any material property. The subscripts f, m, and c denote fiber, matrix, and composite. Fiber/matrix stress transfer is maximized when fibers are aligned with tensile load. Otherwise, an orientation factor (α_o) can be applied. For synthetic fibers, it is reported that three-dimensional random fibre alignment yields to α_o value of 1/5, planar randomly oriented fibers yields to α_o value of 3/8, and load axially aligned fibers yields to α_o value of 1 (Baïlon and Dorlot 2000; Gibson 2007). The 3/8 case was recently confirmed for natural fibers (Beckermann and Pickering 2009).

$$P_c = \alpha_o P_f v_f + P_m v_m \tag{1}$$

The Kelly–Tyson model suggests that the maximum stress in fibers (σ_f) within the composite is proportional to the fiber aspect ratio (L/D) and the fiber/matrix interfacial shear stress (τ), according to the relation $\sigma_f = 2\tau(L/D)$ (Gibson 2007). Incorporating this model into ROM gives the composite tensile strength as a function of fiber aspect ratio Eq. 2 (Baïlon and Dorlot 2000; Gibson 2007).

$$\sigma_c = \alpha_o 2\tau(L/D)v_f + \sigma_m v_m \tag{2}$$

The Cox model suggests that stress in fibers is proportional to the difference between the fiber strain and the hypothetical matrix strain if there were no fibers (Gibson 2007). Equation 3 gives the composite tensile modulus of elasticity (E_c) as a function of fiber length according to the Cox model (Cox 1952; Gibson 2007), where G_m is the matrix shear modulus, A_f is the fiber cross-section area, and D_1 is the distance between two adjacent fibers perpendicular to their axis. An analytical solution for the parameter β, proposed by Kelly, is also given in Eq. 3 (Gibson 2007; Kelly 1973).

$$E_c = E_f\left[1 - \frac{\tanh(\beta L/2)}{(\beta L/2)}\right]v_f + E_m v_m \quad \text{where} \quad \beta^2 = \frac{2\pi G_m}{A_f E_f \ln(D_1/D)} \tag{3}$$

The Halpin–Tsai equation is a semi-empirical model Eq. 4 that accounts for the E_f/E_m ratio and a curve fitting parameter ξ (Gibson 2007). Halpin originally proposed $\xi = 2(L/D)$ for aligned fibers (Gibson 2007; Halpin 1969).

$$E_c = E_m\left(\frac{1+\xi\eta\, v_f}{1-\eta\, v_f}\right) \quad \text{where} \quad \eta = \frac{E_f/E_m - 1}{E_f/E_m + \xi} \tag{4}$$

Materials and methods

Commercial white birch bleached chemico–thermomechanical pulp fibers were used. Three fiber aspect ratio classes (length-to-diameter, *L/D*) were obtained through mechanical refining and screening and characterized with an OpTest fiber quality analyzer (Table 1). Aspect ratios were obtained from fiber arithmetic mean length divided by average diameter. Fiber intrinsic strength (breaking length of handsheet) was measured with a standard zero–span tensile test (TAPPI 1996). Breaking load was 88.3 N. High-density polyethylene (HDPE) LB 0100–00 (Equistar) having a melt index of 0.5 g/10 min, solid density of 953 kg/m^3, tensile strength of 27.3 MPa, and tensile modulus of elasticity (MOE) of 1.172 GPa was used as matrix material. Maleated polyethylene (MAPE) AC–575A (Honeywell) was used as a compatibility agent, and OptiPak OP–100 (Honeywell) was used as a process lubricant.

A Cincinnati Milacron 35 mm conical counter–rotating twin–screw extruder was used to produce extruded samples. A low screw speed of 5 rpm was set to limit fiber breakage. A Sumitomo 55–US ton SE–DU series injection molding machine was used to form injection–molded samples. The detailed procedure is given in Migneault et al. (2009). WPC formulations are presented in Table 1. All composites were processed with 40% wood fiber mass proportion. Extruded composites were

Table 1 Wood-plastic composite (WPC) formulations, densities, and tensile properties (with standard deviations in brackets)

WPC	Fiber *L/D*	Additives	ρ_c (kg/m^3)	σ_c (MPa)	E_c (GPa)
Extrusion					
1	8.3	No additive	1,094 (7)	23.4 (0.2)	2.83 (0.04)
2	13.0		1,080 (9)	24.9 (0.5)	2.96 (0.02)
3	21.3		1,076 (9)	28.2 (0.3)	2.99 (0.02)
4	8.3	MAPE	1,079 (3)	19.0 (1.2)	2.33 (0.11)
5	13.0		1,065 (21)	22.7 (1.8)	2.72 (0.07)
6	21.3		1,084 (7)	24.9 (1.0)	2.79 (0.09)
7	8.3	Lubricant	1,074 (2)	19.2 (1.0)	2.58 (0.06)
8	13.0		1,060 (8)	22.5 (0.8)	2.74 (0.07)
9	21.3		1,065 (5)	24.3 (1.0)	2.75 (0.06)
Injection molding					
10	8.3	MAPE & Lubricant	1,018 (4)	27.3 (0.5)	2.96 (0.03)
11	13.0		1,019 (6)	31.5 (1.4)	3.00 (0.12)
12	21.3		1,016 (2)	36.5 (1.0)	3.18 (0.09)

L/D fiber aspect ratio (length/diameter), ρ_c composite density, σ_c composite tensile strength, E_c composite tensile modulus of elasticity, *MAPE* maleated polyethylene

processed for each fiber aspect ratio class and three different additive levels: no additive, compatibility agent, and process lubricant. Variation in additive type would vary the fiber/matrix adhesion quality, which was considered in the models. Injection molded composites were produced with both compatibility agent and lubricant.

Composite samples were analyzed using an S–3500 N variable pressure vacuum scanning electron microscope (Hitachi). Tensile strength (maximum strength) and modulus of elasticity were measured according to ASTM D 638–03 (specimen type I). Testing speed was 5 mm/min. Six replicates were run for each of the 12 composite formulations (Table 1).

Results and discussion

Composites were processed using mass proportions for experimental convenience. However, volume fractions are required to apply micromechanical models. Volume fractions were obtained from equation set 5 Eq. 5, where m is the mass fraction, v is the volume fraction, and ρ is the density. All calculations were performed assuming that HDPE properties are unchanged after composite formation.

$$\begin{aligned} m_{\mathrm{f}} + m_{\mathrm{m}} &= m_{\mathrm{c}} = 1 \\ v_{\mathrm{f}} + v_{\mathrm{m}} &= v_{\mathrm{c}} = 1 \\ m_{\mathrm{m}} &= \frac{m_{\mathrm{m}}}{m_{\mathrm{c}}} = \frac{\rho_{\mathrm{m}} v_{\mathrm{m}}}{\rho_{\mathrm{c}} v_{\mathrm{c}}} \end{aligned} \tag{5}$$

Wood fraction density in the composites, calculated with the ROM, varies from 1,145 to 1,345 kg/m^3. These values are much higher than the solid density of white birch solid wood (about 500 kg/m^3). This is because the fibers in the composite are collapsed. Fiber intrinsic strength was calculated using zero–span tensile load of 88.1 N, handsheet grammage of 60 g/m^2, and handsheet tensile specimen width of 15 mm. When calculated on the basis of equivalent cell wall area, using cell wall density of 1.5 g/cm^3, fiber strength is 147 MPa. When calculated on the basis of wood fraction density within formed composite, fiber strength varies from 112 to 132 MPa.

Tensile strength

Figure 2 shows WPC tensile strength according to the Kelly–Tyson model Eq. 2 compared with measured strength. The model was fitted to experimental values for injected–molded WPC by adjusting fiber/matrix interfacial shear stress (τ) until the minimum sum of squared error (SSE) was reached (Table 2). SSE is calculated as: $\mathrm{SSE} = \sum_{i=1}^{i=N} (\sigma^i_{\mathrm{model}} - \sigma^i_{\mathrm{experiment}})^2$, where N is the number of fiber L/D levels. A fiber orientation factor of 1 was applied to the injected–molded case because fibers are aligned (Fig. 3a). For the extrusion case, a fiber orientation factor of 3/8 was applied because fibers are randomly oriented (Fig. 3b). Optimized shear stress (obtained at minimum SSE) was the same for aligned and randomly oriented fibers

(1.41 MPa, Table 2). The only difference between the two models presented in Fig. 2 is the fiber orientation factor (α_o). This suggests that the difference between injected–molded and extruded WPC can be explained mainly by fiber orientation, because the 3/8 factor for planar randomly oriented fibers allowed a shift from the aligned to the randomly oriented fibers case. Maximum stress in wood fraction varies from 6.7 to 60.1 MPa (Table 2). As previously reported (Beckermann and Pickering 2009; Doan et al. 2006; Simonsen 1997; Sretenovic et al. 2006), fiber contribution to composite strength is lower than intrinsic fiber strength. It is, in the better case, one half of the intrinsic fiber strength (112 MPa). This result can be explained, in part, by the poor compatibility between polar fibers and non–polar thermoplastic, stress concentrations due to micro-voids, and heterogeneous strain of the different phases (Godara et al. 2009). Consequently, fibers are not broken when the composite breaks, and instead are pulled out, as shown in Fig. 3c.

Using the shear stress found, the critical fiber aspect ratio$(L/D)_c$ (Fig. 1) can be calculated with Eq. 6. For the aligned fiber case, calculated $(L/D)_c$ is 40. This value is below the average size for white birch fibers ($L/D = 68$, Smook 2002). At this $(L/D)_c$, WPC tensile strength would be 54.4 MPa, according to the Kelly–Tyson model Eq. 2.

$$\left(\frac{L}{D}\right)_c = \frac{\sigma_{f,max}}{2\tau} \tag{6}$$

Fiber/matrix shear stress was reduced when a process lubricant was used. This result was expected because the use of a lubricant decreases composite mechanical properties (Li et al. 2004). Unexpectedly, however, the use of a compatibility agent also reduced fiber/matrix shear stress. Determination coefficients between the models and experimental values are close to 1 in all cases (Table 2). This suggests that the variation according to fiber size is linear. Thus, a linear model was appropriate.

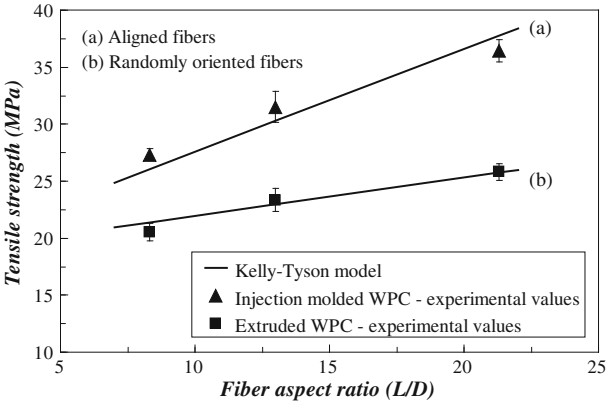

Fig. 2 Comparison between measured and modeled (Kelly–Tyson model) tensile strength of WPC made of HDPE and wood fibers of different aspect ratios (*error bars* represent ± 1 SD)

Table 2 Optimized values used to fit* the Kelly–Tyson model to composite tensile strength

WPC	τ* (MPa)	σ_f (MPa)	SSE	R^2
Extrusion (randomly oriented fibers, $\alpha_o = 3/8$)				
1 to 3	1.97	12.3–31.5	1.09	0.996
4 to 6	1.16	7.2–18.5	3.86	0.912
7 to 9	1.08	6.7–17.3	2.73	0.900
Average (1 to 9)	1.41	8.8–22.5	0.84	0.988
Injection molding (aligned fibers, $\alpha_o = 1$)				
10 to 12	1.41	23.4–60.1	4.81	0.962

* Adjusted to fit the model to experimental values (minimum SSE), τ fiber/matrix interfacial shear stress, σ_f fiber stress, α_o fiber orientation factor, *SSE* sum of squared error, R^2 determination coefficient

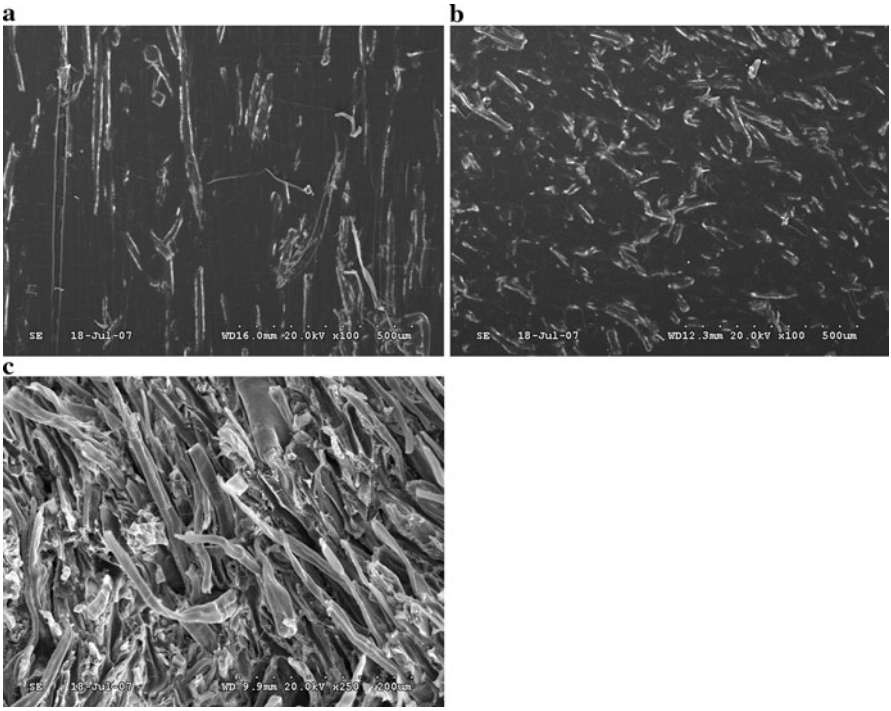

Fig. 3 Micrographs of WPC showing **a** aligned fibers in injected-molded WPC (100× enlargement), **b** randomly oriented fibers in extruded WPC (100× enlargement), and **c** pulled-out fibers on a ruptured surface (250× enlargement)

Tensile modulus of elasticity

Figure 4 shows the tensile modulus of elasticity of the WPC modeled by the Cox model compared to measured tensile values. Equation 3 was re–written as a function of fiber aspect ratio Eq. 7 by incorporating the relations $G_m = E_m/2(1 + \upsilon_m)$ and $A_f = \pi D^2/4$, where υ is Poisson's ratio (0.35 was used for HDPE). Assuming

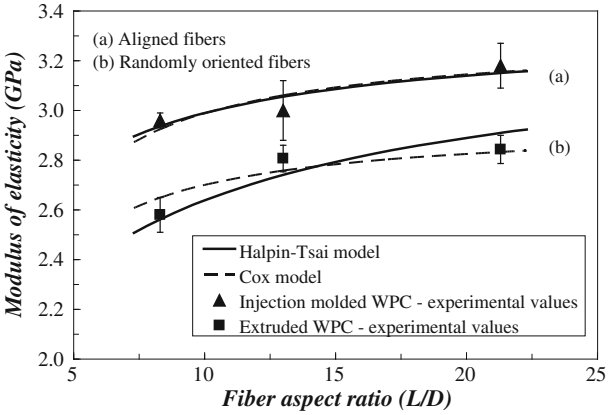

Fig. 4 Comparison between measured and modeled (Halpin–Tsai model or Cox model) tensile modulus of elasticity of WPC made of HDPE and wood fibers of different aspect ratios (*error bars* represent ± 1 SD)

that fibers are at equal axial distance D_1 from each other, and assuming a hexagonally shaped element of matrix material around the fibers, D_1 was expressed as a function of D, according to the relation $D_1 = D\left[(\pi/4\sqrt{3})(v_m/v_f + 1)\right]^{1/2}$.

$$E_c = E_f\left[1 - \frac{\tanh(\beta L/D)}{(\beta L/D)}\right]v_f + E_m v_m \quad \text{where} \quad \beta^2 = \frac{E_m}{E_f(1+v_m)\ln(D_1/D)} \tag{7}$$

The Cox model Eq. 7 was fitted to experimental values for injection molding by adjusting the fiber modulus of elasticity (E_f) until the minimum SSE was reached (Table 3). Previously, an orientation factor of 3/8 allowed shifting from the aligned (injection molding) to the planar randomly oriented (extrusion) fiber case. This factor did not work with the Cox model. Thus, an optimal fiber modulus of elasticity was found for each WPC formulation (Table 3). The modulus of elasticity of the wood fraction within the composite varies between 6.27 and 8.84 GPa. These values are lower than those reported in the literature for pulp fibers (about 20–40 GPa, Mark et al. 2002).

Figure 4 shows the tensile modulus of elasticity of the WPC modeled by the Halpin–Tsai model Eq. 4 compared to measured tensile values. The model was fitted to experimental values by adjusting E_f until the minimum SSE was reached (Table 3). As for tensile strength, an orientation factor of 3/8 was applied, allowing a shift from the aligned to the random orientation case (Fig. 4). The 3/8 factor was applied to the curve fitting parameter ξ. The optimized E_f value for the two cases is almost the same (7.84 vs. 7.91). This suggests, as was proposed for tensile strength with the Kelly–Tyson model, that the difference in tensile modulus between extruded and injection–molded WPC can be explained mainly by fiber orientation.

Comparison of model performance

Figure 5 shows the relationship between modeled tensile properties and measured values for all composite formulations. Correlation is closer for tensile strength

Table 3 Optimized values used to fit* the Cox model and the Halpin–Tsai model to the composite tensile modulus of elasticity

WPC	Cox model			Halpin–Tsai model			
	E_f* (GPa)	SSE ($\times 10^{-3}$)	R^2	E_f* (GPa)	α_o	SSE ($\times 10^{-3}$)	R^2
Extrusion (randomly oriented fibers)							
1 to 3	7.38	1.9	0.943	8.84	3/8	38	0.892
4 to 6	6.27	58	0.926	7.20	3/8	29	0.876
7 to 9	6.52	2.3	0.873	7.51	3/8	15	0.810
Average (1 to 9)	6.73	7.2	0.919	7.84	3/8	9.0	0.865
Injection molding (aligned fibers)							
10 to 12	7.83	5.6	0.804	7.91	1	4.5	0.836

* Adjusted to fit the model to experimental values (minimum SSE), E_f fiber modulus of elasticity, α_o fiber orientation factor, *SSE* sum of squared error, R^2 determination coefficient

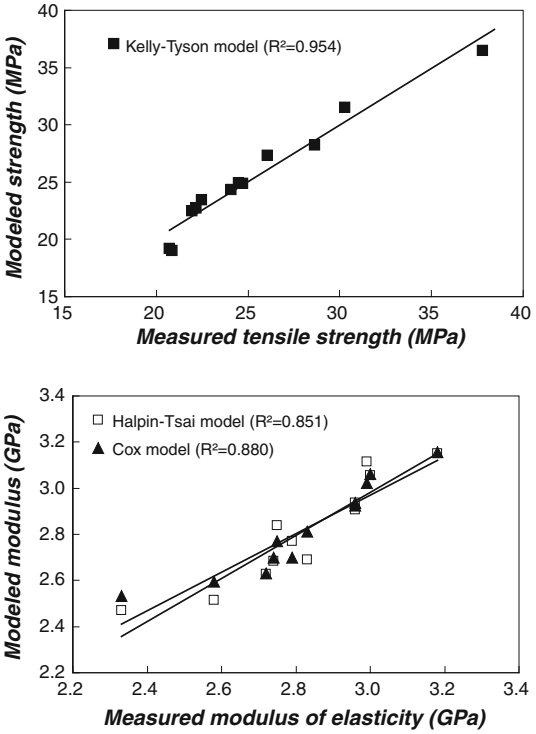

Fig. 5 Relationship between measured and modeled tensile properties for all composite formulations

($R^2 = 0.954$) than tensile modulus of elasticity ($R^2 = 0.851$–0.880). For modulus of elasticity, the determination coefficient is higher for the Cox than the Halpin–Tsai model. Moreover, SSE is mostly smaller with the Cox than the Halpin–Tsai model (Table 3). These results show that the Cox model is more appropriate for this study. However, the Halpin–Tsai model gives a better response with the fiber orientation

factor. For the aligned fibers case, the two models are almost superposed (Fig. 4). Finally, it is interesting to note that the models were appropriate for a wide range of values, especially for tensile strength (Fig. 5).

Although models presented in this study fitted to experimental values, they have some limitations. For example, they assume isotropic and linear elastic materials. In fact, the tensile behavior of wood and HDPE is not perfectly linear elastic and wood fibers are orthotropic (Marklund et al. 2008). Models also represent fibers as perfectly straight cylinders. In fact, wood fibers are empty shaped (lumen) and also are collapsed. Average values of aspect ratios were used. However, each aspect ratio class contains a distribution of lengths and diameters. Finally, models were fitted to experimental values, but were not able to predict composite tensile properties.

Conclusion

Wood–plastic composites (WPC) were processed using fibers of different aspect ratio (length-to-diameter, *L*/*D*), different processing methods, and different additives. Tensile properties of WPC were measured and modeled as a function of fiber aspect ratios. The models applied to tensile strength (Kelly–Tyson model) and tensile modulus of elasticity (Cox model and Halpin–Tsai models) showed good fit to experimental values. A shift was achieved from the oriented fiber case (injection molding) to the randomly oriented fiber case (extrusion) using a fiber orientation factor of 3/8 for both tensile strength and modulus of elasticity. This suggests that fiber orientation is the main factor responsible for the difference between the tensile properties of WPC made with the two processes. Fiber/matrix stress transfer increased with increasing fiber aspect ratio. Stress transfer was reduced with the use of process lubricant. Unexpectedly, the compatibility agent had the same effect. Fiber strength and stiffness contributions to the composite were lower than those of intrinsic fiber properties.

Acknowledgments The authors are grateful to the Canada Research Chair Program, the Ministère du développement économique et de l'innovation et de l'Exportation (MDEIE) du Québec, NSERC, Caisse Populaire Desjardins, Tembec, and the UQAT Foundation for financial support. The authors wish to thank Professor Michael Wolcott and Dr. Karl Englund from Washington State University for granting access to the Wood Engineering Material Laboratory and for their collaboration on this project.

References

Baïlon JP, Dorlot JM (2000) Des matériaux, troisième édition. Presses Internationales Polytechnique, Montréal

Beckermann GW, Pickering KL (2009) Engineering and evaluation of hemp fibre reinforced polypropylene composites: micro-mechanics and strength prediction modelling. Composites Part A 40:210–217

Clemons C (2002) Wood-plastic composites in the United States-The interfacing of two industries. Forest Prod J 52(6):10–18

Cox HL (1952) The elasticity and strength of paper and other fibrous materials. Br J Appl Phys 3:72–79

Doan TTL, Gao SL, Mäder E (2006) Jute/polypropylene composites I. Effect of matrix modification. Compos Sci Technol 66:952–963

Gibson RF (2007) Principles of composite material mechanics. CRC Press, New York
Godara A, Raabe D, Bergmann I, Putz R, Müller U (2009) Influence of additives on the global mechanical behavior and the microscopic strain localization in wood reinforced polypropylene composites during tensile deformation investigated using digital image correlation. Compos Sci Technol 69:139–146
Halpin JC (1969) Stiffness and expansion estimates for oriented short fiber composites. J Compos Mater 3:732–734
Herra-Franco PJ, Valadez-González A (2005) A study of the mechanical properties of short natural-fiber reinforced composites. Composites Part B 36:597–608
Kalaprasad G, Joseph K, Thomas S, Pavithran C (1997) Theoretical modelling of tensile properties of short sisal fibre-reinforced low-density polyethylene composites. J Mater Sci 32:4261–4267
Kelly A (1973) Strong solids, vol 2. Clarendon Press, Oxford
Li H, Law S, Sain M (2004) Process rheology and mechanical property correlationship of wood flour-polypropylene composites. J Reinf Plast Compos 23(11):1153–1158
Mark RE, Habeger CC, Borch J, Lyne BM, Murakami K (2002) Handbook of physical testing of paper, vol 1, 2nd edn. Marcel Dekker, New York
Marklund E, Varna J, Neagu CR, Gamstedt KE (2008) Stiffness of aligned wood fiber composites: effect of microstructure and phase properties. J Compos Mater 42(22):2377–2405
Migneault S, Koubaa A, Erchiqui F, Chaala A, Englund K, Wolcott MP (2009) Effects of processing method and fiber size on the structure and properties of wood–plastic composites. Composites Part A 40:80–85
Neagu CR, Gamstedt KE, Berthold F (2006) Stiffness contribution of various wood fibers to composite materials. J Compos Mater 40(8):663–698
TAPPI (1996) Zero–span breaking strength of pulp (dry zero–span tensile). Standard T 231 cm–96. Technical association of the pulp and paper industry, Atlanta
Rowell RM (2007) Challenges in biomass–thermoplastic composites. J Polym Environ 15:229–235
Simonsen J (1997) Efficiency of reinforcing materials in filled polymer composites. Forest Prod J 47(1):74–81
Smith PM, Wolcott MP (2006) Opportunities for wood/natural fiber–plastic composites in residential and industrial applications. Forest Prod J 56(3):4–11
Smook GA (2002) Handbook for pulp & paper technologists, 3rd edn. Angus Wilde publications, Vancouver
Sretenovic A, Müller U, Gindl W (2006) Mechanism of stress transfer in a single wood fibre–LDPE composite by means of electronic laser speckle interferometry. Composites Part A 37(9):1406–1412